PHYSICAL REVIEW B **77**, 100506(R) (2008)

Doping dependence of the vortex-core energy in bilayer films of cuprates

L. Benfatto,[1,2] C. Castellani,[2] and T. Giamarchi[3]

[1]*Centro Studi e Ricerche "Enrico Fermi," Via Panisperna 89/A, I-00184 Rome, Italy*

[2]*CNR-SMC-INFM and Department of Physics, University of Rome "La Sapienza," Piazzale Aldo Moro 5, 00185 Rome, Italy*

[3]*DPMC-MaNEP, University of Geneva, 24 Quai Ernest-Ansermet, CH-1211 Genève 4, Switzerland*

(Received 10 December 2007; revised manuscript received 12 February 2008; published 17 March 2008)

The energy needed to create a vortex core is the basic ingredient to address the physics of thermal vortex fluctuations in underdoped cuprates. Here, we theoretically investigate its role in the occurrence of the Beresinskii-Kosterlitz-Thouless transition in a bilayer film with inhomogeneity. From the comparison with recent measurements of the penetration depth in two-unit-cell thin films, we can extract the value of the vortex-core energy μ and show that μ scales linearly with T_c at low doping.

DOI: 10.1103/PhysRevB.77.100506 PACS number(s): 74.20.−z, 74.78.Bz, 74.72.−h

One of the most puzzling aspects in the physics of high-temperature superconductors (HTSCs), which makes them substantially different from conventional superconductors, is the separation between the fundamental energy scales associated with superconductivity: the critical temperature T_c, the zero-temperature superconducting (SC) gap Δ, and the superfluid stiffness $J_s=\hbar^2\rho_s d_\perp/4m$.[1] Here, ρ_s is the superfluid density, measured through the London penetration depth λ, and $\rho_s d_\perp$ is an effective two-dimensional superfluid density, where $d_\perp$ is a characteristic transverse length scale (see discussion below). While in a BCS superconductor the gap formation and the appearance of superfluid currents happen simultaneously at T_c, with $\Delta \sim T_c$, in the HTSC at low doping level the two phenomena are essentially decoupled, and $T_c \sim J_s$. This suggests that the transition can be controlled by phase fluctuations, described within an effective XY model for the phase degrees of freedom, where J_s sets the scale of the phase coupling. On a general ground, also the energetic cost μ needed to create the vortex core is connected to λ^{-2}, i.e., to J_s. Using standard BCS relations, one can see that at $T=0$ both J_s and μ are of the order of the Fermi energy, which is a large energy scale compared to T_c. Nonetheless, in thin films of conventional superconductors, $J_s(T)$ goes to zero as T approaches T_{BCS}, and $\mu(T) \sim J_s(T)$ is reduced, so that vortex creation becomes possible but only at a T_c very near to T_{BCS}.

In underdoped cuprate superconductors, where the BCS picture fails, a clear understanding of the typical energy scale that controls the vortex-core formation is still lacking. In particular, despite the fact that several experiments[2,3] suggest a predominant role of vortex fluctuations,[4] whose occurrence is controlled in a crucial way by the value of μ,[5–8] not much attention has been devoted yet to characterize the vortex-core energy μ and its relation with T_c. In this Rapid Communication, we propose a procedure to estimate μ using penetration-depth measurements in thin films. Indeed, in this case, the transition is ultimately of Beresinkii-Kosterlitz-Thouless (BKT) type, as it is signaled by the linear relation between T_c and J_s, and its persistence as doping is changed by the electric-field effect[9,10] or chemical doping.[11] To clarify the role played by the vortex-core energy, let us recall some basic features of the BKT physics in a SC film made of few unit cells. In Y-based cuprates, whose data we will analyze below, there are two strongly coupled CuO_2 layers within each cell, which will be considered in what follows as the basic two-dimensional (2D) unit of the layered system, of thickness $d=12$ Å, corresponding to the unit-cell size in the c direction. Then, for an n-cell-thick SC film, one would expect the system to behave as an effective two-dimensional (2D) superconductor with areal density $\rho_s^{2D}=nd\rho_s$, where ρ_s is the three-dimensional superfluid density connected to the penetration depth λ. The energy scale to be compared to the temperature is then

$$J_n=\frac{\hbar^2\rho_s^{2D}}{4m}=\frac{nd\hbar^2\rho_s}{4m}=\frac{nd}{\lambda^2}\frac{\Phi_0^2}{4\pi^2\mu_0}, \qquad (1)$$

where $\Phi_0=(h/2e)$ is the flux quantum and μ_0 the vacuum permittivity; we used MKS units as in Ref. 11. According to the BKT theory, a transition is expected when J_n/T equals the universal value $2/\pi$, which gives the following relation in terms of $1/\lambda^2(T)$:

$$0.62\times\frac{nd\,[\text{Å}]}{\lambda^2(T^n_{BKT})[\mu m^2]}=\frac{2}{\pi}T^n_{BKT}[K]. \qquad (2)$$

This approach assumes that all the layers of the film are so strongly coupled that no mismatch of the SC phase in neighboring layers is possible, i.e., the film behaves as an effective 2D layer of total thickness nd. However, in the case of cuprates, it is well known that the intercell Josephson coupling $J_\perp$ is very weak, so that except in a narrow region around T_c one expects to see the BKT behavior of a *single* unit cell. As far as the superfluid-density behavior is concerned, one will then expect that the superfluid density has already dropped when Eq. (2) with $n=1$ is satisfied, which is certainly the case for totally uncoupled cells. The best situation to analyze this effect in real systems is provided by the finite-frequency sheet conductivity measurements of thin $Y_{1-x}Ca_xBa_2Cu_3O_{7-\delta}$ (YBCO) films by Hetel *et al.*[11] Indeed, in these two-unit-cell thick samples, the superfluid-density downturn is necessarily between $T^{n=1}_{BKT}$ and $T^{n=2}_{BKT}$, and its exact form depends on the relative strength of $J_\perp$ and vortex-core energy. As we shall see, this allows us to extract from the data of Ref. 11 the doping dependence of the vortex-core energy.

As a starting point, we need a model for the BKT SC transition in the two-layer system where, for simplicity, we denote a single unit cell of the sample with "layer" in the following. By adopting the formal analogy between quantum one-dimensional (1D) and thermal 2D systems,[6,12] we describe each layer (labeled with the subscript 1,2, respectively) as a quantum 1D sine-Gordon model [$\int \equiv \int dx v_s/(2\pi)$],

$$H_{1,2} = H^0_{1,2} - \frac{g_u}{a^2}\int \cos(2\phi_{1,2}), \tag{3}$$

$$H^0 = \int \left[K(\partial_x \theta_{1,2})^2 + \frac{1}{K}(\partial_x \phi_{1,2})^2 \right]. \tag{4}$$

Here, θ_i represent the SC phases, ϕ_i are the conjugate fields, with $[\theta_i(x'), \partial_x \phi_j(x)] = i\pi\delta_{ij}\delta(x'-x)$, K is the Luttinger-liquid parameter, g_u is the strength of the sine-Gordon potential, a is the short-distance cutoff, and v_s is the velocity of 1D fermions (which is immaterial in the 1D-2D mapping where $v_s\tau$ plays the role of the second spatial dimension,[6,12] τ being the imaginary time). A vortex configuration for the θ variable requires that $\oint \nabla\theta = \pm 2\pi$ over a closed loop, i.e., the creation of a 2π kink, generated by the exponential of its conjugate field, the operator $e^{i\phi}$.[12] Thus, the parameter K defines the superfluid stiffness and g_u, the vortex fugacity, as

$$K \equiv \frac{\pi J}{T}, \quad g_u = 2\pi e^{-\beta\mu}, \tag{5}$$

where $J \equiv J_{n=1}$ is the single-layer stiffness. Within the standard 2D *XY* model for the phase, the vortex-core energy μ is controlled by J itself,[5,13]

$$\mu_{XY} = \pi J \ln(2\sqrt{2}e^{\gamma}) \simeq \frac{\pi^2}{2}J, \tag{6}$$

where γ is the Euler's constant. Even though we will treat μ as an *independent* parameter to be fixed by comparison with the experiments, for the sake of clarity we will measure it in multiples of μ_{XY}. The effect of the Josephson coupling $J_\perp$ is accounted for by the term

$$H_\perp = -\frac{g_\perp}{a^2}\int \cos(\theta_1 - \theta_2), \tag{7}$$

where $g_\perp = \pi J_\perp / T$. As we shall see below, the interlayer coupling is relevant under renormalization group (RG) flow and tends to lock the phases in neighboring layers. When this effect dominates over the vortex unbinding, the superfluid density is not affected by crossing $T^{n=1}_{BKT}$. As T increases further an additional coupling generated under RG flow becomes relevant and induces the 2D transition at $T^{n=2}_{BKT}$. It corresponds to the formation of a vortex simultaneously in two layers,

$$\frac{g_s}{a^2}\int \cos[2(\phi_1 + \phi_2)]. \tag{8}$$

It is then clear that a more convenient basis to study the system is given by the symmetric/antisymmetric fields, $\theta_{s,a} = (\theta_1 \pm \theta_2)/\sqrt{2}$. The full Hamiltonian then becomes

$$H = H^0_a(K_a) + H^0_s(K_s) + \frac{4g_u}{a^2}\int \cos(\sqrt{2}\phi_s)\cos(\sqrt{2}\phi_a) - \frac{2g_\perp}{a^2}\int \cos(\sqrt{2}\theta_a) + \frac{2g_s}{a^2}\int \cos(2\sqrt{2}\phi_s), \tag{9}$$

where H^0 is defined in Eq. (4), $K_{s,a} = K$, and the initial value of g_s is zero, even though it is generated at $\mathcal{O}(g_u^2)$ under RG flow [see Eq. (15) below]. The superfluid density J_s is connected to the second-order derivative of the free energy with respect to an infinitesimal twist δ of the phase, $\partial_x\theta_i \to \partial_x\theta_i - \delta$. Since the θ_a field is unchanged by this transformation while $\partial_x\theta_s \to \partial_x\theta_s - \sqrt{2}\delta$, we immediately see that J_s is given by the asymptotic value of $K_s(\ell)$ under RG flow,

$$J_s \equiv \frac{\hbar^2 \rho_s^{2D}}{4m} = \frac{K_s(\ell\to\infty)T}{\pi}. \tag{10}$$

The perturbative RG equations for the couplings K_a, K_s, g_u, $g_\perp$, and g_s can be derived by means of the operator product expansion. The result is (see also Refs. [6,14–16])

$$\frac{dK_a}{d\ell} = 2g_\perp^2 - K_a^2 g_u^2, \tag{11}$$

$$\frac{dg_u}{d\ell} = \left(2 - \frac{K_a + K_s}{2}\right)g_u - g_u g_s K_s, \tag{12}$$

$$\frac{dK_s}{d\ell} = -g_u^2 K_s^2 - 2g_s^2 K_s^2, \tag{13}$$

$$\frac{dg_\perp}{d\ell} = \left(2 - \frac{1}{2K_a}\right)g_\perp, \tag{14}$$

$$\frac{dg_s}{d\ell} = (2 - 2K_s)g_s + \frac{1}{2}g_u^2(K_s - K_a), \tag{15}$$

with $\ell = \log(a/a_0)$, where a_0 and a are the original and RG rescaled lattice spacings, respectively. Equations (11)–(15) share many similarities with the multilayer case discussed in Ref. 6. If the layers are uncoupled ($g_\perp = 0$), then $K_s = K_a$ at all scales, and the transition occurs when g_u flows to a strong coupling. This happens at $K_s = 2$, which corresponds to $T^{n=1}_{BKT}$ according to definitions (1), (2), and (5). However, when the layers are coupled, $g_\perp$ grows under RG flow, even if it initially has a small value. If the bare couplings—which are T dependent—are such that $g_\perp$ becomes of order 1 before g_u is, the Josephson coupling term will lock the relative phase θ_a in neighboring layers and g_u will flow to zero even if $K_s < 2$. However, as soon as $K_s = 2$, the g_s coupling becomes relevant, signaling the simultaneous vortex formation in the two layers. These effects make g_u relevant as well, and the superfluid stiffness K_s jumps suddenly from the value $K_s = 1$ at $T^{n=2}_{BKT}$ to zero.

As discussed in Ref. 6, the range of temperature above $T^{n=1}_{BKT}$ where the interlayer coupling allows the system to sustain a finite superfluid density, is *not* universal and depends

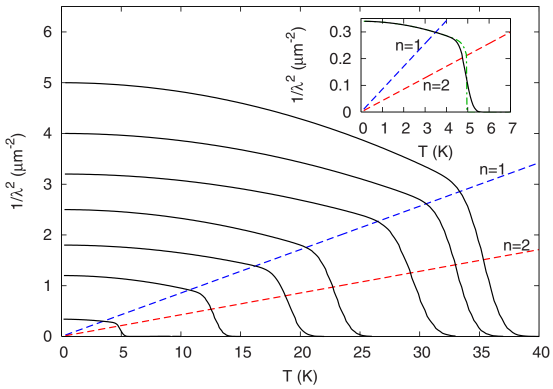

FIG. 1. (Color online) Temperature dependence of the superfluid density in the inhomogeneous bilayer system, with parameter values explained in the text. The downturn is located at the intersection with the line $n=1$ or $n=2$ for uncoupled or totally coupled layers, respectively. Inset: expanded view for the most underdoped case. The dashed-dotted line is the result obtained without averaging over the J_0 inhomogeneity.

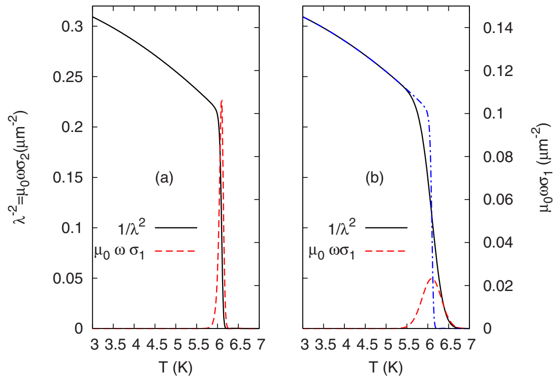

FIG. 2. (Color online) (a) $1/\lambda^2$ and $\mu_0\omega\sigma_1$ evaluated at $\omega=50$ kHz for a single $\bar{J}(T)$ curve (here, $\mu=3\mu_{XY}$). The finite frequency leads to a sharp but continuous decrease of $1/\lambda^2$ across T_{BKT}, along with a peak in σ_1. (b) $1/\lambda^2$ and $\mu_0\omega\sigma_1$ evaluated at finite frequency using the averaged J_{inh}. Also shown for comparison is the homogeneous curve of panel (a) (dashed-dotted line).

crucially on the value of the vortex-core energy, which sets the initial value of the fugacity g_u [see Eq. (5)]. Thus, at small μ the system will display a rapid downturn already at $T_{BKT}^{n=1}$, followed by an abrupt jump at $T_{BKT}^{n=2}$, while for large values of μ we expect to see only the signature of the two-layer BKT transition at $T_{BKT}^{n=2}$. This is indeed what we observe in the experimental data of Ref. 11. While at higher dopings ($25\text{ K}<T_c<40\text{ K}$) the superfluid density shows a clear downturn already at $T_{BKT}^{n=1}$, as the doping is decreased further this signature disappears and only the BKT jump at $T_{BKT}^{n=2}$ is visible (see the inset of Fig. 1). To have a quantitative estimate of μ, we calculated J_s by a numerical integration of Eqs. (11)–(15), stopped at a scale ℓ^* where $g_\perp=s\sim\mathcal{O}(1)$ (we used $s=3$) to account for the perturbative character of the RG equations. The bare temperature dependence of the superfluid density mimics the low-T behavior of the data, $J(T)=J(T=0)-\alpha T^2$, with $J(T=0)$ and α extracted from the experimental data well below the transition. We also assume that $J_\perp/J$ is independent of doping, and we choose $J_\perp/J=10^{-3}$, which is appropriate in the range of doping considered.[17] Thus, the only remaining free parameter is μ, which can be chosen by fitting the temperature dependence of the data around the transition. The result, reported in Fig. 1 as $\lambda^{-2}(T)$, is in excellent agreement with the data of Ref. 11.

According to the previous discussion, at $T_{BKT}^{n=2}$ the superfluid density should display a BKT jump, while the data of Ref. 11 show clearly a broad tail around the estimated $T_{BKT}^{n=2}$. This effect, along with the temperature dependence of the real part of the conductivity, cannot be attributed only to the finite frequency of the measurements. Instead, the simplest explanation is the existence of a T_c inhomogeneity in the sample, which we accounted for in the fit of Fig. 1. To clarify this point, let us discuss for simplicity the pure 2D case for a two-layer thick film. In this case, after a transient regime the RG flow of Eqs. (11)–(15) is simplified to

$$\frac{dK_s}{d\ell}=-2K_s^2g_s^2, \quad \frac{dg_s}{d\ell}=(2-2K_s)g_s, \tag{16}$$

with a fixed point at $K_s=1$, which corresponds to $T_{BKT}^{n=2}$ in Eq. (2). The complex conductivity $\sigma=\sigma_1+i\sigma_2$ at a finite frequency ω is given by

$$\sigma(\omega)=-\frac{1}{\lambda^2e^2\mu_0}\frac{1}{i\omega\varepsilon(\omega)}, \tag{17}$$

where $\varepsilon(\omega)=\varepsilon^1+i\varepsilon^2$ is a complex dielectric constant due to bound and free vortex excitations. Following the dynamical theory of Ambegaokar *et al.*[18] and Halperin and Nelson,[19] we estimate these two contributions by using the RG flow [Eq. (16)] of the BKT couplings and by evaluating $\epsilon(\omega)$ at the finite scale $\ell_\omega=\log(r_\omega/a)$. Here, $r_\omega=\sqrt{14D/\omega}$ is the maximum length probed by the oscillating field, where $D\sim\hbar/m=10^{16}$ Å/s is the diffusion constant of vortices and ω the frequency of the measurements. According to Eqs. (17) and (1), $\lambda^{-2}=\mu_0\omega\sigma_2$. Due to the finite frequency, the jump of λ^{-2} expected in the $\omega=0$ case is replaced by a sharp but continuous drop in a range ΔT_ω above $T_{BKT}^{n=2}$. At the same time, σ_1 acquires a finite value, with a peak of approximately the same width ΔT_ω. However, using the value $\omega=50$ KHz corresponding to the experiments of Ref. 11 the rounding effect on λ^{-2} and the peak width in σ_1, reported in Fig. 2(a), are still much smaller than what are measured experimentally. A more reasonable explanation for the large transient region is the sample inhomogeneity. Such inhomogeneity is also suggested by tunneling measurements in other families of cuprates,[20] where approximately Gaussian fluctuations of the local gap value are observed. Even though the issue of the microscopic origin of this effect is beyond the scope of this Rapid Communication, we nonetheless find that an analogous distribution of the superfluid-stiffness J_0 values around a given $\bar{J}$ can account very well for the data of Ref. 11. Thus, we compare with the experiments the quantity $J_{inh}(T)=\int dJ_0P(J_0)J(T,J_0)$, where each $J(T,J_0)$ curve is obtained from the RG equations [Eqs. (11)–(15)] using a bare superfluid stiffness $J=J_0-\alpha T^2$. Each initial value J_0 has a probability $P(J_0)=\exp[-(J_0-\bar{J}_0)^2/2\sigma^2](\sqrt{2\pi}\sigma)$ of being realized, where the bare average stiffness $\bar{J}(T)=\bar{J}_0-\alpha T^2$ has $\bar{J}_0$ and α fixed by the experimental data at low T, where $J_{\rm expt}(T)$ is practically the same as $\bar{J}(T)$. However, using a variance $\sigma=0.05\bar{J}_0$, we obtain a very good agreement with the experiments near the transition, as far as both the tail of λ^{-2} and the position and width of $\sigma^1(\omega)$ are concerned [see Fig. 2(b)]. Observe also that such a variance can be compatible, within an intermediate-coupling scheme for the superconductivity, with the few times larger distribution of gap values ($\sigma\approx 0.15\bar{\Delta}$) reported in tunneling experiments.[20]

The same finite-frequency analysis is made more involved in the bilayer case because the RG equations [Eqs. (11)–(15)] should be stopped at scales smaller than ℓ_ω to prevent the flow of the $g_\perp$ at strong coupling. Thus, in Fig. 1, we included only the effect of the T_c inhomogeneity by means of the average over $P(J_0)$ discussed above (with $\sigma=0.06\bar{J}_0$ for the most underdoped samples). This procedure accounts very well for the long tails of λ^{-2} above the transition (see inset) without affecting significantly the estimate of μ.

Let us now comment on the doping dependence of $\mu(T=0)$ reported in Fig. 3. As we have said, the measured T_c crosses over from approximately $T_{BKT}^{n=1}$ at high doping to $T_{BKT}^{n=2}$ at low doping. This is reflected in the doping dependence of μ/μ_{XY}: Indeed, as we observed for the multilayer case,[6] as μ increases with respect to the single-layer stiffness J, the transition moves away from $T_{BKT}^{n=1}$. It is worth noting that since T_c is controlled by the competition between the vortex fugacity and the interlayer coupling, in principle, the crossover of T_c from $T_{BKT}^{n=1}$ to $T_{BKT}^{n=2}$ could be obtained also by keeping μ fixed and by varying $J_\perp$. However, to reproduce the data, we should assume in this case an unlikely increase in $J_\perp$ by 2 orders of magnitude as the doping is decreased up to $J_\perp/J\sim 10^{-1}$. Despite the nonuniversal behavior of μ/μ_{XY}, the absolute value of μ reported in Fig. 3(b) scales linearly with T_c.

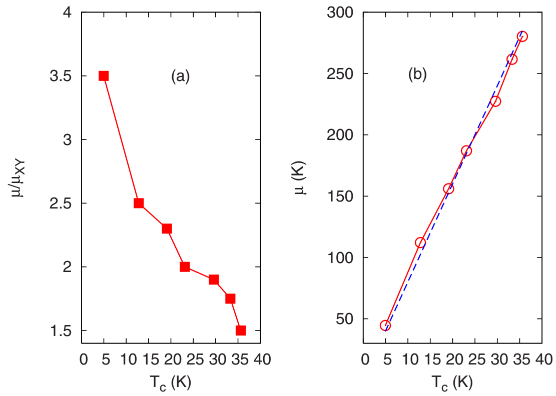

FIG. 3. (Color online) Vortex-core energy as a function of T_c extracted from the fit in Fig. 1. (a) Ratio between μ and the μ_{XY} value [Eq. (6)], proportional to the single-layer energy J. (b) Absolute value of μ in K. The dashed line is $\mu=8T_c$.

This is our central result, which establishes a precise relation between the vortex-core energy and T_c in severely underdoped cuprate superconductors.

In summary, we analyzed the occurrence of the BKT transition in a bilayer system. By means of the RG approach, we computed the temperature dependence of the superfluid stiffness of the bilayer, and we proved the crucial role played by the vortex-core energy μ in controlling the transition. Taking into account also the sample inhomogeneity, we provided an excellent fit of the experimental data of Ref. 11, which allowed us to extract a linear scaling of μ with T_c in underdoped YBCO. A theoretical understanding of this result is still lacking, and no doubt it would constitute a stringent test of microscopic proposals for the underdoped phase.

This work was supported in part by MIUR PRIN 2005, Prot. 2005022492, and by the Swiss NSF under MaNEP and Division II.

[1] P. A. Lee, N. Nagaosa, and X.-G. Wen, Rev. Mod. Phys. **78**, 17 (2006).
[2] Y. Wang, L. Li, and N. P. Ong, Phys. Rev. B **73**, 024510 (2006).
[3] L. Li, J. G. Checkelsky, S. Komiya, Y. Ando, and N. P. Ong, Nat. Phys. **3**, 311 (2007).
[4] Z. Tešanović, arXiv:0705.3836, Nature-Physics (to be published).
[5] P. Minnaghen, Rev. Mod. Phys. **59**, 1001 (1987).
[6] L. Benfatto, C. Castellani, and T. Giamarchi, Phys. Rev. Lett. **98**, 117008 (2007).
[7] L. Benfatto, C. Castellani, and T. Giamarchi, Phys. Rev. Lett. **99**, 207002 (2007).
[8] S. Raghu, D. Podolsky, A. Vishwanath, and D. A. Huse, arXiv:0801.2925 (unpublished).
[9] A. Rüfenacht, J.-P. Locquet, J. Fompeyrine, D. Caimi, and P. Martinoli, Phys. Rev. Lett. **96**, 227002 (2006).
[10] D. Matthey, N. Reyren, J.-M. Triscone, and T. Schneider, Phys. Rev. Lett. **98**, 057002 (2007).
[11] I. Hetel, T. R. Lemberger, and M. Randeria, Nat. Phys. **3**, 700 (2007).
[12] T. Giamarchi, *Quantum Physics in One Dimension* (Oxford University Press, Oxford, 2004).
[13] J. M. Kosterlitz and D. J. Thouless, J. Phys. C **6**, 1181 (1973).
[14] P. Donohue and T. Giamarchi, Phys. Rev. B **63**, 180508(R) (2001).
[15] L. Mathey, A. Polkonikov, and A. H. C. Neto, Europhys. Lett. **81**, 10008 (2007).
[16] M. A. Cazalilla, A. Iucci, and T. Giamarchi, Phys. Rev. A **75**, 051603(R) (2007).
[17] A. Hosseini, D. M. Broun, D. E. Sheehy, T. P. Davis, M. Franz, W. N. Hardy, R. Liang, and D. A. Bonn, Phys. Rev. Lett. **93**, 107003 (2004).
[18] V. Ambegaokar, B. I. Halperin, D. R. Nelson, and E. D. Siggia, Phys. Rev. B **21**, 1806 (1980).
[19] B. I. Halperin and D. R. Nelson, J. Low Temp. Phys. **36**, 599 (1979).
[20] K. K. Gomes, A. N. Pasupathy, A. Pushp, S. Ono, Y. Ando, and A. Yazdani, Nature (London) **447**, 569 (2007).